Please cite this article in press as: Dong et al., Spatiomechanical Modulation of EphB4-ephrin-B2 Signaling in Neural Stem Cell Differentiation, Biophysical Journal (2018), https://doi.org/10.1016/j.bpj.2018.06.031

Biophysical *Journal*
Article

Biophysical Society

Spatiomechanical Modulation of EphB4-ephrin-B2 Signaling in Neural Stem Cell Differentiation

Meimei Dong,[1,2] Dawn P. Spelke,[3,4] Young Kwang Lee,[1] Jean K. Chung,[1] Cheng-Han Yu,[5] David V. Schaffer,[3,4,*] and Jay T. Groves[1,2,*]

[1]Department of Chemistry, [2]Biophysics Graduate Group, [3]Department of Chemical Engineering, and [4]Department of Bioengineering, University of California Berkeley, Berkeley, California; and [5]Mechanobiology Institute, National University of Singapore, Singapore, Singapore

ABSTRACT Interactions between EphB4 receptor tyrosine kinases and their membrane-bound ephrin-B2 ligands on apposed cells play a regulatory role in neural stem cell differentiation. With both receptor and ligand constrained to move within the membranes of their respective cells, this signaling system inevitably experiences spatial confinement and mechanical forces in conjunction with receptor-ligand binding. In this study, we reconstitute the EphB4-ephrin-B2 juxtacrine signaling geometry using a supported-lipid-bilayer system presenting laterally mobile and monomeric ephrin-B2 ligands to live neural stem cells. This experimental platform successfully reconstitutes EphB4-ephrin-B2 binding, lateral clustering, downstream signaling activation, and neuronal differentiation, all in a configuration that preserves the spatiomechanical aspects of the natural juxtacrine signaling geometry. Additionally, the supported bilayer system allows control of lateral movement and clustering of the receptor-ligand complexes through patterns of physical barriers to lateral diffusion fabricated onto the underlying substrate. The results from this study reveal a distinct spatiomechanical effect on the ability of EphB4-ephrin-B2 signaling to induce neuronal differentiation. These observations parallel similar studies of the EphA2-ephrin-A1 system in a very different biological context, suggesting that such spatiomechanical regulation may be a common feature of Eph-ephrin signaling.

INTRODUCTION

Eph receptors (EphA1-8,10 and EphB1-4,6) constitute the largest family of receptor tyrosine kinases, and their membrane-bound ephrin ligands are either glycophosphatidylinositol-linked A-type (ephrinA1-10) or transmembrane B-type (ephrinB1-3) proteins. Eph-ephrin interactions thus occur between apposed cells, with bidirectional signaling in some cases (1,2). These juxtacrine cues play an integral role in normal developmental processes such as tissue patterning (3) and axonal pathfinding (4), as well as in abnormal pathological conditions such as developmental disorders and cancer (5,6).

Eph receptors are a unique class of receptor tyrosine kinases for which activity requires not only Eph dimerization and transphosphorylation but also multivalent oligomerization into higher-order clusters to initiate downstream signaling (7,8). Furthermore, Eph receptors can exhibit homotypic and heterotypic *cis*-interactions in addition to intercellular *trans*-interactions with various Ephs and ephrins to form complex signaling clusters (2,9). Eph signaling cluster size, composition, spatial organization, and mechanical forces have all been identified as possible modulators of Eph signaling and the resultant functional cellular outcomes (10,11). In particular, mechanical sensitivity and spatial organization of cell surface receptors are increasingly recognized as relevant cellular stimuli (12–16). For instance, when EphA2-ephrin-A1 signaling cluster movement is physically restricted, proximal membrane signaling events including recruitment of the downstream signaling effector ADAM10 (17) and ephrin-A1 trans-endocytosis (18) are markedly altered.

A particularly important system in which Eph-ephrin signaling has been widely studied is neural development, in which downstream signal transduction controls neural stem cell (NSC) proliferation, migration, and survival both during early development and in adulthood (19–21). Furthermore, Eph-ephrin signaling was recently demonstrated to regulate hippocampal neurogenesis in the adult brain, where ephrin-B2 expressed by astrocytes in the NSC niche induces the neuronal differentiation of NSCs

Submitted November 7, 2017, and accepted for publication June 6, 2018.

*Correspondence: schaffer@berkeley.edu or jtgroves@lbl.gov

Meimei Dong and Dawn P. Spelke contributed equally to this work.

Cheng-Han Yu's present address is School of Biomedical Sciences, Li Ka Shing Faculty of Medicine, The University of Hong Kong, Pok Fu Lam, Hong Kong.

Editor: Valentin Nagerl.

https://doi.org/10.1016/j.bpj.2018.06.031

Please cite this article in press as: Dong et al., Spatiomechanical Modulation of EphB4-ephrin-B2 Signaling in Neural Stem Cell Differentiation, Biophysical Journal (2018), https://doi.org/10.1016/j.bpj.2018.06.031

via EphB4 signaling (22,23). The process of NSC-mediated adult neurogenesis plays important roles in learning, memory, and neurological disease (24–28). Structural experiments have confirmed that ephrin-B2 binds EphB4 receptors to form heterodimers (29), and a recent study has shown increased downstream activity in NSCs with increasingly multivalent ephrin-B2 ligands (23). Thus, biophysical mechanisms of receptor activation likely play a vital role in this therapeutically relevant system. Motivated by the work on the spatiomechanical sensitivity of the EphA2 receptor and the regulatory role of the EphB4 receptor in NSC signaling, we hypothesized that NSC differentiation may be sensitive to spatial manipulation of EphB4-ephrin-B2 physical organization and clustering.

Previous studies have induced EphB4 signaling by artificially preclustering ephrin-B2 in solution to generate multimeric receptor-ligand complexes (22,23). However, these methods do not recapitulate the physical interactions between membrane-bound receptors and ligands. We therefore turned to supported lipid bilayers (SLBs), a system well suited for studying cell-cell contact-dependent signaling (15,17,30–33). Here, we develop a hybrid system to reconstitute the juxtacrine signaling geometry between NSCs and astrocytes by depositing EphB4 receptor-expressing NSCs onto SLBs displaying laterally mobile, monomeric ephrin-B2 ligands. This system provides a physiologically and spatially relevant microenvironment for studying EphB4-ephrin-B2 signaling. It also allows us to precisely control not only the chemical composition of the ligands and membranes but also the physical geometry of receptor-ligand complexes using the technique of spatial mutation (34). Spatial mutation involves the physical control of the spatial patterning of proteins on a lipid bilayer achieved by nanofabricating metal structures on the underlying glass substrates (35,36). The resulting features guide the movement of supported membrane molecules as well as any engaged cognate receptors on the live cell, thereby controlling the cluster size and number of receptor-ligand complexes that can form (32,37,38). Any cellular microenvironmental perturbation, including the spatial mutation, that alters the movement of cell-surface molecules intrinsically imposes mechanical forces onto the cell. Cellular responses to such perturbations are thus spatiomechanically regulated. This, however, does not imply that the receptor system involved directly senses mechanical force.

Using this reconstituted juxtacrine signaling platform, we observe EphB4-ephrin-B2 co-clustering and demonstrate membrane-bound monomeric ephrin-B2 activation of EphB4 signaling and downstream neuronal differentiation. Furthermore, by employing spatial mutation, we discover that EphB4 signaling and NSC differentiation are spatially and potentially mechanically modulated. Restricting the motion of supported membrane ephrin-B2 within arrays of small ($\sim$1 μm) grid-patterned corrals was sufficient to abrogate its effects on NSC differentiation, even though similar levels of ephrin-B2 were available to the cell. This result is similar to the spatiomechanical regulation observed in the EphA2-ephrin-A1 system (17,18), suggesting that such effects may be general to other Eph-ephrin interactions within the family. This work suggests that physical aspects of the NSC niche may impact differentiation and further indicates that this may be significant in the context of regenerative medicine.

MATERIALS AND METHODS

The extracellular domain of mouse ephrin-B2 was cloned into a pFastBac vector containing the SNAP-tag and His10 sequences and then introduced into the bac-to-bac insect cell baculovirus-based expression system. Ephrin-B2-SNAPtag-His10 fusion protein was secreted from infected Sf9 cells, purified by Ni-NTA resin, and then eluted using an imidazole gradient. NSCs were isolated from the hippocampi of adult female Fisher 344 rats and cultured on polyornithine- and laminin-coated tissue-culture plates. NSCs were grown in 1:1 Dulbecco's modified Eagle's medium/F12 with N-2 supplement and recombinant human FGF-2. The EphB4-mCherry NSC line was engineered through stable retroviral infection. Imaging experiments were performed on a Nikon Eclipse Ti-E/B motorized inverted microscope (Nikon, Tokyo, Japan). Micromanager and imageJ were used to collect, analyze, and process images. FCS measurements were performed on a home-built spectrometer integrated into a Nikon TE2000 inverted microscope.

RESULTS

Development of a DNA-SNAP-tag functionalization strategy

To investigate the effect of monomeric membrane-bound ephrin-B2-induced signaling on NSC differentiation, we developed a DNA-SNAP-tag biochemical conjugation method to tether ephrin-B2 ligands to a SLB for extended presentation. This development was motivated by the fact the conventional NiNTA-His-tag membrane-linkage strategy (18,39), which we have previously used with ephrin-A1, has limited stability (e.g., 1–2 h) under normal cell-culture conditions. DNA oligonucleotides are a versatile tool for protein conjugation because hybridization of complementary DNA strands is highly specific and sensitive (40). DNA linkage also offers the possibility of controlling formation of ligand heterodimers or even larger clusters (41), though these capabilities are not needed in this study.

SNAP-tag, a 20 kDa mutant of the DNA repair protein O^6-alkylguanine-DNA alkyltransferase, has been widely used to functionalize proteins via a site-specific irreversible covalent reaction with a benzylguanine (BG) substrate (42,43). In step one, a fusion protein of the extracellular domain of ephrin-B2 and SNAP-tag was recombinantly produced and then covalently conjugated to a 20 basepair single-stranded (ss) DNA (Seq1) oligonucleotide through an irreversible BG-SNAP interaction to form a protein-DNA complex unit. This conjugated ssDNA was covalently coupled with a BG substrate on the 5′ end for SNAP-tag chemistry and was covalently linked to Cy5 on the 3′ end

Please cite this article in press as: Dong et al., Spatiomechanical Modulation of EphB4-ephrin-B2 Signaling in Neural Stem Cell Differentiation, Biophysical Journal (2018), https://doi.org/10.1016/j.bpj.2018.06.031

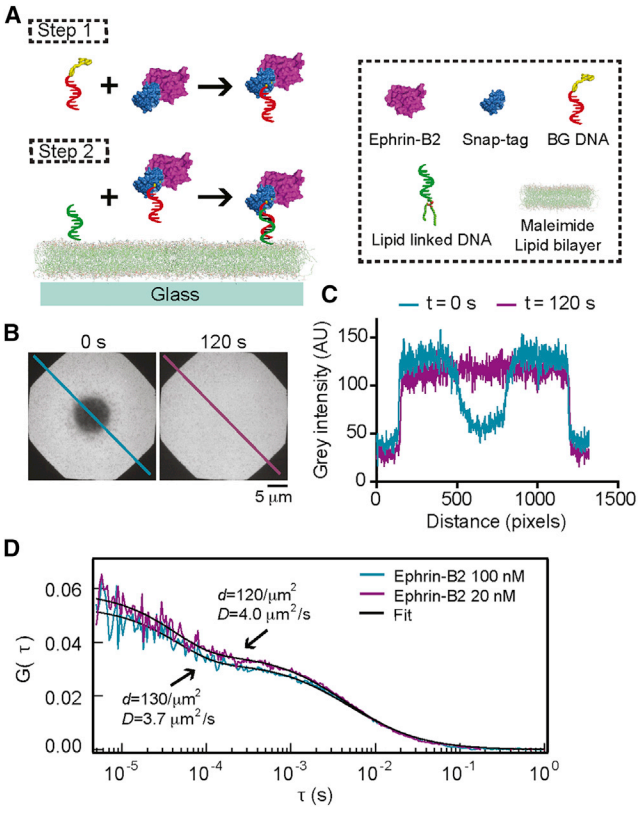

FIGURE 1 Functionalization of DNAs and ephrin-B2-SNAP-tag onto SLB. (*A*) A schematic of a two-step conjugation to tether DNAs and ephrin-B2 ligands onto SLB is shown. In step 1, an ephrin-B2-SNAP-tag is conjugated to Cy5-BG modified ssDNA. In step 2, thiol-modified ssDNA is bound to a maleimide-decorated DOPE lipid bilayer and then hybridized with ephrin-B2-DNA complex. (*B*) Fluorescence recovery after photobleaching (FRAP) characterization of ephrin-B2-displaying SLB is shown. A region of the SLB was bleached for 1 min with a 647 nm epifluorescent light source. Images were captured every 30 s after photobleaching, with representative images at 0 and 120 s. (*C*) A fluorescent intensity analysis of a line scan in (*B*) verified the lateral mobility of the ephrin-B2 linked to the membrane. (*D*) Characterization of ephrin-B2-SLB surface properties is shown. Fluorescence correlations spectroscopy (FCS) was used to determine the physical properties of the membrane-bound ephrin-B2, and the resulting autocorrelation $G_0(\tau)$ was fitted to a two-dimensional Gaussian diffusion model. Incubating with 20 nM ephrin-B2 resulted in a diffusion coefficient of $D = 4.0\ \mu m^2/s$ and a ligand surface density of $\sigma = 120/\mu m^2$.

for fluorescent imaging (Fig. 1 *A*). In step two, a thiol-modified complementary ssDNA (Seq2) oligonucleotide was functionalized to a maleimide-linked membrane, allowing for subsequent hybridization with ephrin-B2-SNAP-tag-DNA (Seq1) and immobilization of the fusion protein onto the bilayer (Fig. 1 *A*). The fluidity of the bilayer and the mobility of ephrin-B2 were confirmed by fluorescence recovery after photobleaching (FRAP) experiments (Fig. 1, *B* and *C*). To further characterize the membrane density of ephrin-B2 ligands, we applied fluorescence correlation spectroscopy (FCS) analysis (44), and a typical time autocorrelation function of fluorescence intensity fluctuations from membrane-bound ephrin-B2 is shown in Fig. 1 *D*. Analysis yielded an observed ephrin-B2 ligand density of $120/\mu m^2$ with a diffusion coefficient of 4.0 $\mu m^2/s$, results that are very consistent with lipid diffusion on supported membranes (45,46). Of note, in the FCS experiments, we tested the ligand surface densities of two solution concentrations of ephrin-B2 and obtained similar values for both the membrane ephrin-B2 density and the diffusion coefficient (Fig. 1 *D*). We thus concluded that we had reached the saturation point for ligand binding to the SLB. Importantly, this strategy enables ephrin-B2 ligands to remain stably attached to the membrane for periods of 12–24 h under normal cell culture conditions.

NSCs cluster membrane-bound monomeric ephrin-B2

To reconstitute the juxtacrine geometry of Eph-ephrin signaling, we seeded NSCs on ephrin-B2 functionalized SLBs (Fig. 2 *A*). Utilizing total internal reflection fluorescence (TIRF) microscopy, we recorded live NSC interactions with the bilayer (Video S1), and time-lapse images demonstrated the spatial distribution and cluster formation of ephrin-B2 at the NSC-SLB interface. Upon NSC landing, membrane-bound ephrin-B2 diffused rapidly and immediately formed microclusters with the cell; these microclusters continued to move inward and eventually stabilized into a large centralized cluster within 45 min. Reflection interference contrast microscopy (RICM) images were taken to map the footprint (contact areas) of cells on the underlying SLB, and the contact area domain showed strong colocalization with ephrin-B2 clusters (Fig. 2 *B*). Cells failed to adhere to bilayers that lacked ephrin-B2, confirming that the only linkages between NSCs and the SLBs were through ephrin-B2 ligands.

EphB4 serves as a key transducer of ephrin-B2 induced neurogenesis in NSCs (22). To investigate whether the formation of ephrin-B2 microclusters on SLBs was due to interactions with EphB4 receptors, an NSC line stably expressing an EphB4-mCherry fusion was developed and then seeded on ephrin-B2 SLBs. Employing confocal microscopy, we observed the three-dimensional membrane distribution of EphB4 on NSCs. The resulting confocal images depict the distribution of exogenous EphB4-mCherry receptors on the NSCs membrane, which reflects that of the membrane distribution of endogenous EphB4 receptors in NSCs (22). These confocal images also demonstrated the colocalization of ephrin-B2 and EphB4 binding at the bilayer-cell membrane interface (Fig. 2 *C*; Fig. S1). Colocalization of ephrin-B2 and EphB4 was also verified by TIRF microscopy at initial cell-membrane contact stage and 45 min post-cell landing (Fig. S2; Video S2). Together with previous FCS data (Fig. 1 *D*), this suggests that bilayer ephrin densities are roughly similar to receptor densities on NSCs. Blocking EphB4 receptors on NSCs

Please cite this article in press as: Dong et al., Spatiomechanical Modulation of EphB4-ephrin-B2 Signaling in Neural Stem Cell Differentiation, Biophysical Journal (2018), https://doi.org/10.1016/j.bpj.2018.06.031

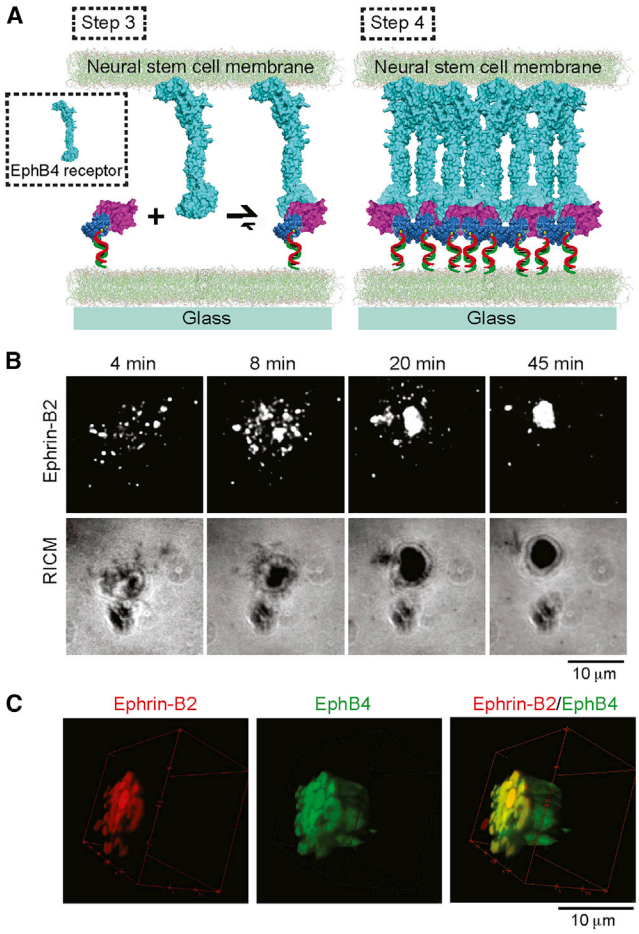

FIGURE 2 Reconstitution of EphB4-ephrin-B2 signaling junction at SLB-cell interface. (*A*) A schematic of an NSC interacting with ephrin-B2 ligands on an SLB is given. (*B*) Time-lapse RICM and TIRF images showed a representative NSC landing and clustering with ephrin-B2. Cy5-BG-DNA-conjugated ephrin-B2-SNAP ligands visualized by TIRF microscopy (*top*) are shown; cell adhesion imaged by RICM (*bottom*). Post-seeding, NSCs were imaged over 45 min. At 4 min, the RICM image showed cells weakly adhered on SLB. Ephrin-B2 diffused and formed sparse microscopic clusters. Over time, ephrin-B2 continued to cluster, and cell adhesion to SLB strengthened. 45 min later, a centralized large micron-scale ephrin-B2 cluster was formed. (*C*) Confocal three-dimensional images of an EphB4-mCherry expressing NSC interacting with an ephrin-B2 SLB 45 min after seeding are shown. EphB4-ephrin-B2 colocalization at the NSC-SLB interface is apparent.

by incubation with an EphB4 antibody before seeding resulted in a significant drop in the number of cells attached to SLBs, but did not eliminate adhesion completely, suggesting that other Ephs such as EphB2, which also binds ephrin-B2 (47), may be involved in this interaction. Blocking EphB2 receptors resulted in decreased NSC binding but to a lesser degree than EphB4 blocking, whereas preblocking both EphB4 and EphB2 receptors resulted in adhesion levels similar to EphB4 blocking (Fig. S3). These observations indicate that multiple Ephs, but predominantly EphB4, are responsible for NSC adhesion to the SLBs.

NSCs undergo neuronal differentiation on ephrin-B2 SLBs

To examine the biological activity of our reconstituted EphB4-ephrin-B2 signaling system, we studied the differentiation of NCSs cultured on ephrin-B2 SLBs. In general, SLBs can provide stable presentation of a ligand for 1–2 h using conventional NiNTA-His-tag membrane linkage strategy, after which the SLB begins to deteriorate (ligand dissociation) (18,39). In contrast, the SNAP-tag functionalization strategy developed here allows for stable ephrin-B2 tethering for 24 h. Culturing NSCs for the 5 days required for a cell to complete initial stages of its differentiation also necessitated functionalization of the culture surface to support cell adhesion post-bilayer degradation. The bilayer began to disintegrate and was no longer intact after ~24 h post cell seeding. For NCSs to grow on SLBs for 5 days, culture media was supplemented 18 h post-seeding with laminin, a standard extracellular matrix protein used for NSC culture (22,23). As controls (nonbilayer studies), NSCs were seeded in standard tissue culture conditions on laminin-coated glass substrates and exposed to a naïve condition (FGF-2-supplemented media), a media condition that induced differentiation into a mixture of neurons and astrocytes (retinoic acid + fetal bovine serum (RA/FBS), or mixed differentiation media), or media conditions containing antibody clustered soluble ephrin-B2 (Fc-ephrin-B2) for 1 and 5 days. Fc-ephrin-B2 is a recombinant form of the ephrin-B2 ectodomain fused to an Fc moiety that can be clustered with an anti-Fc antibody to form a bioactive ephrin-B2 multimer. Preclustering Fc-ephrin ligands in solution has been previously used as a means to trigger Eph-ephrin clustering, and previous studies have shown preclustered Fc-ephrinB2 in solution can trigger neuronal differentiation in NSCs (7,8).

Neuronal differentiation was assessed 5 days postseeding. In standard culture wells, NSCs continuously exposed to RA/FBS or clustered Fc-ephrin-B2 for 5 days underwent high levels of neuronal differentiation (35.7% ± 2.19 and 28.7% ± 4.91, respectively), as measured by the percent of cells expressing the neuronal marker βIII-tubulin. In contrast, a single dose of Fc-ephrin-B2 at the time of seeding had no effect on differentiation. Intriguingly, NSCs on ephrin-B2 bilayers exhibited neuronal differentiation at levels similar to continuous RA/FBS and Fc-ephrin-B2 exposure (36.7% ± 5.78) (Fig. 3 *A*). Morphologically, neurons differentiating after exposure to membrane-bound ephrin-B2 had two to five branching βIII-tubulin^{+} processes, which closely resembled Fc-ephrin-B2-induced neurons (Fig. 3 *B*). Notably, in contrast to the Fc-ephrin-B2 condition in which cells were continuously exposed to the clustered soluble ligand, NSCs on SLBs were only exposed to the ephrin-B2 present on the bilayer from the time of seeding until SLB deterioration 24 h later.

Please cite this article in press as: Dong et al., Spatiomechanical Modulation of EphB4-ephrin-B2 Signaling in Neural Stem Cell Differentiation, Biophysical Journal (2018), https://doi.org/10.1016/j.bpj.2018.06.031

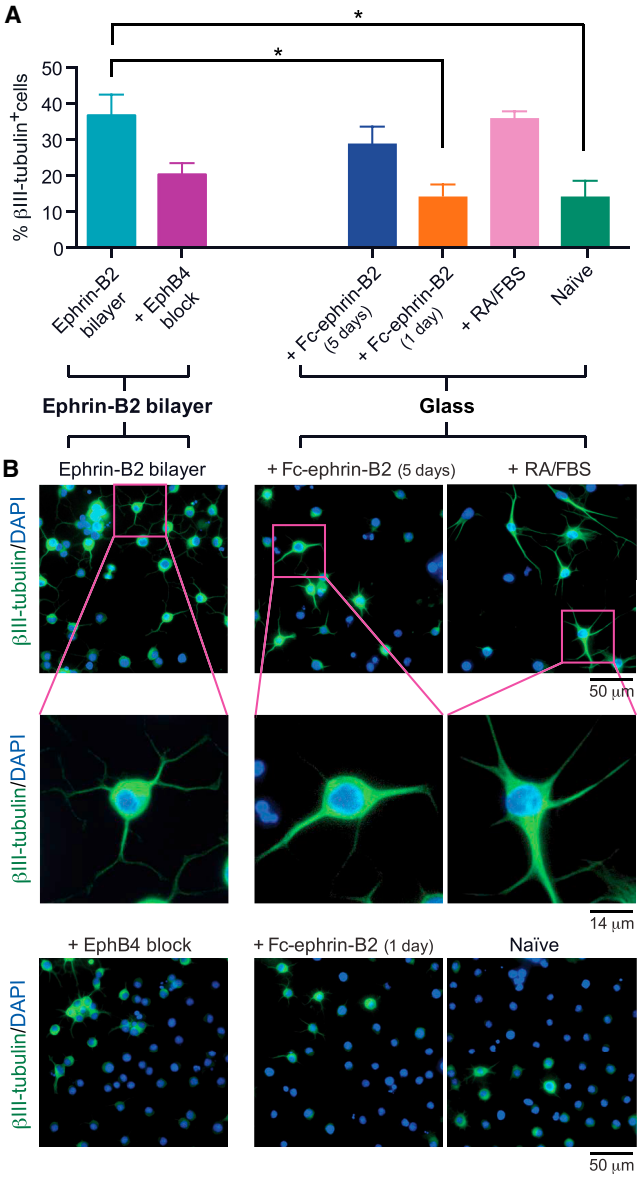

FIGURE 3 NSCs undergo neuronal differentiation due to membrane-bound ephrin-B2. (*A*) Quantification of neuronal differentiation 5 days postseeding by immunostaining as measured by the percentage of NSCs expressing neuronal marker βIII-tubulin is shown. NSCs were cultured on ephrin-B2 SLBs with or without preblocking with an anti-EphB4 antibody followed by laminin addition 1 day postseeding or on laminin-coated glass under naïve, mixed differentiation (RA/FBS), or soluble antibody-clustered Fc-ephrin-B2 (for 1 or 5 days) conditions. Error bars represent the standard error of the mean. $*P < 0.05$, ANOVA with Tukey-Kramer multiple comparison, n = 3 experimental replicates. (*B*) Representative fluorescent images from (*A*) showing neuronal processes (βIII-tubulin+, *green*) and total nuclei (DAPI, *blue*) are shown.

Yet this signal was sufficiently strong enough to induce neuronal differentiation, unlike the single dose of the soluble Fc-ephrin-B2. Finally, to study the role of EphB4, NSCs were incubated with an EphB4 antibody before seeding on SLBs. EphB4-blocked NSCs still adhered to the SLBs, but neuronal differentiation was reduced. The resulting percentage of βIII-tubulin$^+$ cells decreased (20.3% ± 3.18) (Fig. 3 *A*), and induced neurons developed fewer processes (Fig. 3 *B*), confirming the role of EphB4 in transducing ephrin-B2 stimulation. In sum, these findings demonstrate the functional role of membrane-bound monomeric ephrin-B2 ligands in inducing neuronal differentiation.

Spatial mutation impairs cluster formation but not immediate downstream signaling

A spatial mutation experiment, in which patterned supported membranes are utilized to alter the movement and assembly of cell surface receptors, has been successfully applied to investigate spatial organization in immunological synapses (14,32,48,49) and more recently in EphA receptor signaling (17,18,50) and cadherin adhesion (15) but has not been utilized to investigate the role of spatially controlled ligand presentation on a cell fate decision. In the NSC experiments described here, we apply the spatial mutation method by nanofabricating chromium (Cr) metal lines on glass substrates before SLB deposition. The Cr lines serve as diffusion barriers that physically partition the supported bilayer into separate corrals (Fig. 5 *A*) (35,36). As a result, membrane-bound molecules (i.e., ephrin-B2) can only diffuse within each lipid corral, as movement across the Cr barriers is entirely blocked (Fig. 4 *A*). FRAP experiments confirmed that ephrin-B2 diffusion was constrained within corrals, and no transport across barriers was observed (Fig. 4, *B* and *C*).

NSCs seeded on grid-patterned membranes engage ephrin-B2, but movement and assembly of the EphB4-ephrin-B2 signaling clusters is restricted by the underlying grid pattern. On all substrates, NSCs landed and adhered, with similar adhesion areas regardless of patterning. 45 min after NSC seeding, EphB4-ephrin-B2 clusters formed but were confined by 2 and 4 μm spaced grid patterns (Fig. 4 *D*). To rule out any potential artifacts introduced by the Cr grid, a control with similar Cr coverage area to that of the gridded patterns was included in spatial mutation experiments. The control consisted of a substrate patterned with an array of posts spaced 2 μm apart, which allowed ephrin-B2 to freely diffuse around the Cr features. NSCs seeded on these control 2 μm array SLBs induced ephrin-B2 clustering similar to NSCs on nonpatterned SLBs (Figs. 2 *B* and 4 *D*).

Grid patterning the ephrin-B2 membrane did not interfere with activation of EphB4 and immediate downstream signaling. Specifically, pan-phosphorylated-tyrosine and known EphB4-ephrin-B2 signaling targets, including phosphorylated-ERK (51) and active β-catenin (22), were examined. Ephrin-B2 induced signaling was observed in NSCs seeded on nonpatterned (off-grid), 2 μm control-arrayed, 3 μm gridded, and 5 μm gridded ephrin-B2 SLBs, but not on ephrin-B2-free (plain) SLBs (Fig. 4 *E*).

Please cite this article in press as: Dong et al., Spatiomechanical Modulation of EphB4-ephrin-B2 Signaling in Neural Stem Cell Differentiation, Biophysical Journal (2018), https://doi.org/10.1016/j.bpj.2018.06.031

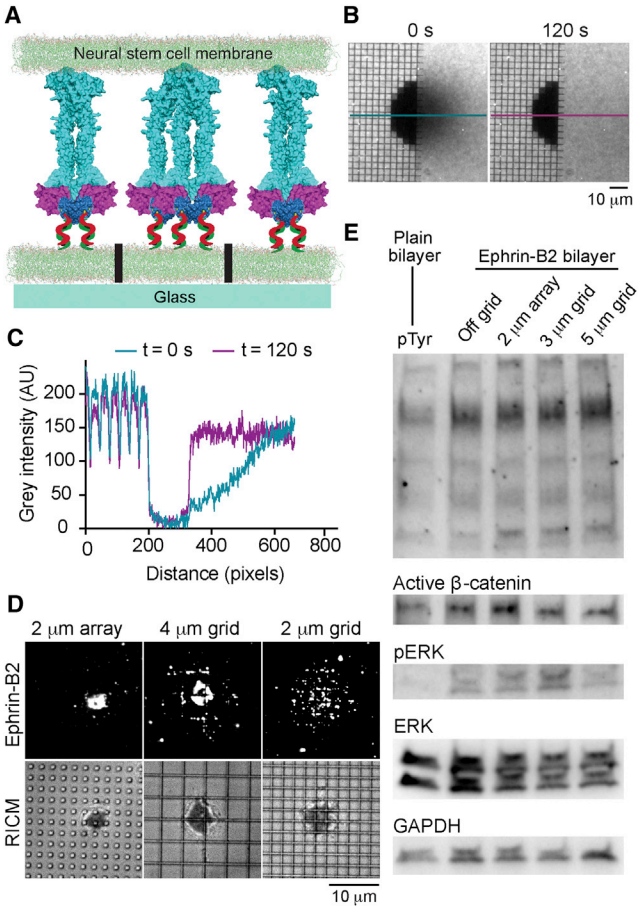

FIGURE 4 Spatial mutation impairs ephrin-B2 clustering but does not affect immediate downstream signaling. (*A*) A schematic of the spatial mutation strategy is shown. An NSC expressing EphB4 interacts with an SLB displaying ephrin-B2. Cr diffusion barriers physically perturb EphB4 receptor movement and cluster formation. (*B*) FRAP characterization of an SLB formed on a nanofabricated 4-μm-spaced gridded substrate is shown. A region of the bilayer at the pattern edge was photobleached with 647 nm epifluorescent light as shown at 0 s. After 120 s, a recovery image was taken. (*C*) Line-scan intensity measurements of (*B*) were taken across the bleached area. Only the nongridded areas were able to recover after photobleaching. (*D*) Ephrin-B2 clustering is disrupted on 4- and 2-μm-spaced gridded substrates, as diffusion is confined to corralled regions. 2 μm arrayed substrates permit diffusion around posts so a central cluster still forms. Cy5-labeled ephrin-B2 visualized by TIRF microscopy (*top*) is shown; cell footprint, RICM (*bottom*). (*E*) Western blots of NSCs after 1 h incubation on plain SLBs, ephrin-B2 SLBs, and patterned ephrin-B2 SLBs (3 and 5 μm) are shown. Pan-phosphotyrosine, active β-catenin, and phosphorylated ERK levels increased on all ephrin-B2 SLBs. ERK and GAPDH were used as loading controls. Quantification of immunoblots is shown in Fig. S5.

Spatial mutation inhibits NSC neuronal differentiation on ephrin-B2 SLBs

The goal of the spatial mutation experiment is to use different grid sizes to titrate the large-scale clustering and organization of EphB4-ephrin-B2 signaling complexes and to test whether spatially impaired clustering impacts cellular signaling in NSCs. Five days postseeding, NSC differentiation was analyzed. NSCs underwent neuronal differentiation at similar levels on unpatterned SLBs, the control array of unconnected metal dots, and on large 5-μm grid-patterned SLBs. However, NSCs exhibited impaired neurogenesis when cultured on smaller grid spacings (3 μm in the experiment shown here). The percent of βIII-tubulin$^+$ cells significantly decreased, and neural processes did not develop (Fig. 5). Therefore, although immediate downstream signaling is not affected by spatial mutation, NSC differentiation mediated by ephrin-B2 signaling is sensitive to the spatial and mechanical properties of ligand presentation in the apposing membrane on the scale of microns. Our observations from the spatial mutation experiments have shown that 3 μm is where the cutoff is for an effect on ephrin-B2-mediated NSCs differentiation.

DISCUSSION

The spatial properties of receptor-ligand interactions can influence receptor activation and signal propagation, but studying this phenomenon requires the development of systems capable of recapitulating complex biophysical traits. In this study, we simulated the juxtacrine geometry of Eph-ephrin signaling transduced by ephrin-B2-presenting astrocytes in contact with EphB4-expressing NSCs (22). By displaying laterally mobile monomeric ephrin-B2 on SLBs, we mimicked the membrane presentation of ephrin-B2. Furthermore, we were able to probe the role of membrane receptor spatial organization in NSC signaling and differentiation using the technique of spatial mutation. The key technical advance enabling these days-long studies was the development of a DNA-SNAP-tag conjugation method providing stable ligand presentation for the duration of bilayer stability. In our hands, bilayers remained intact for 12–24 h.

Because differentiation is a multiday process, it was not known whether 12–24 h of ephrin-B2 presentation on the membrane would be sufficient to induce neurogenesis. Surprisingly, 5 days postseeding, NSCs underwent neuronal differentiation at levels similar to NSCs continuously stimulated with Fc-antibody clustered soluble ephrin-B2. By comparison, however, a 1-day pulse of soluble ephrin-B2 was not sufficient to induce neuronal differentiation. Although ephrin-B2 concentrations cannot be directly compared between soluble and membrane-bound forms, the differentiation results reveal that ligand presentation on a two-dimensional membrane provided much stronger signal strength compared to three-dimensional solution presentation. These findings also suggest that neurogenesis is induced as a result of early signaling decisions initiated through Eph-ephrin interactions.

Ephs and ephrins are known to exhibit a high level of cross talk among family members, so ephrin-B2 on SLBs may interact with other Eph types on NSCs. Indeed, antibody blocking experiments suggested that both EphB4 and EphB2 were responsible for NSC binding, but as concurrent

Please cite this article in press as: Dong et al., Spatiomechanical Modulation of EphB4-ephrin-B2 Signaling in Neural Stem Cell Differentiation, Biophysical Journal (2018), https://doi.org/10.1016/j.bpj.2018.06.031

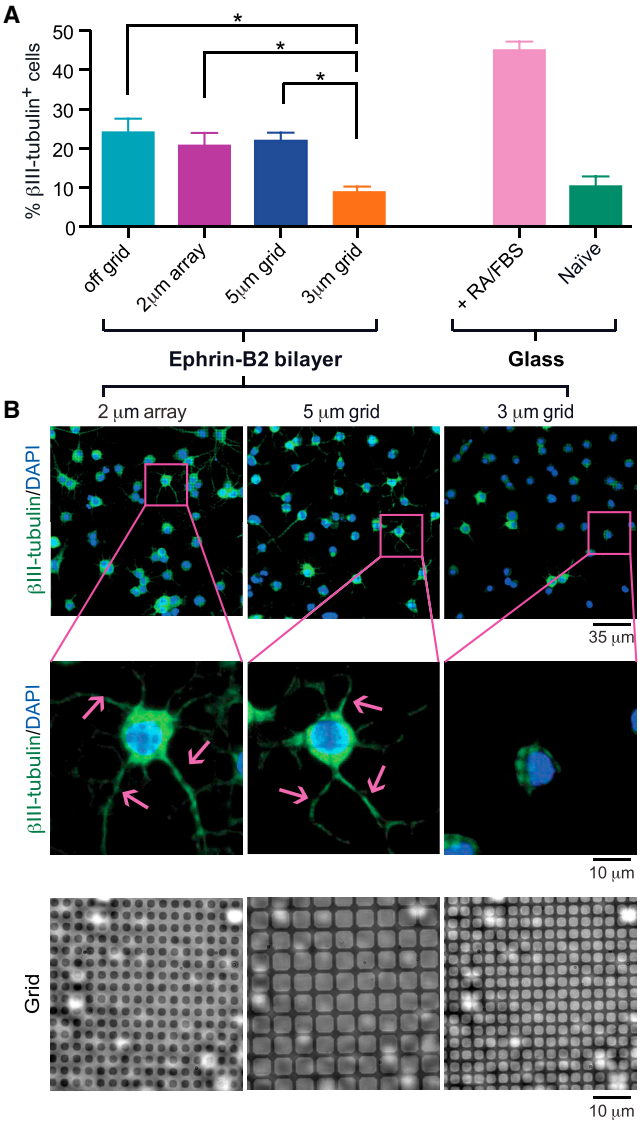

FIGURE 5 Spatial mutation of EphB4 receptors inhibits NSC neuronal differentiation on ephrin-B2 SLBs. (*A*) Quantification of neuronal differentiation by βIII-tubulin expression is shown. NSCs were cultured on off-grid ephrin-B2 SLBs, corral-patterned SLBs, or on standard coverslips under naïve or mixed differentiation conditions. Laminin was supplemented after 1 day for all bilayer conditions, including all substrate-patterned bilayers. Error bars represent standard error of the mean. $*P < 0.05$, ANOVA with Tukey-Kramer multiple comparison, $n = 4$ experimental replicates. (*B*) Representative fluorescent images from (*A*) showing fields of NSCs (*top*), a magnified cell (*middle*), and brightfield images of grid substrates for patterned SLB conditions are shown. Pink arrows mark βIII-tubulin$^+$ neuronal processes.

blocking did not completely ablate adhesion, other Ephs were likely interacting as well. In addition to EphB4 and EphB2, ephrin-B2 has been shown to bind EphB1 (52), EphB3 (53), EphB6 (54), and EphA4 (55). However, EphB4 was confirmed to be largely responsible for transducing the biological activity of ephrin-B2 signaling, as blocking EphB4 abrogated neuronal differentiation (22).

Using this system, we characterized the spatiomechanical sensitivity of EphB4-ephrin-B2 signaling on induced NSC neurogenesis. On 3-μm grid-patterned substrates but not 5 μm grids or nongrid control patterns, neurogenesis was significantly reduced. Importantly, the patterned substrates all presented roughly the same density of ephrin-B2, and Cr grids served only as diffusion barriers to restrict the movement of lipid molecules and ephrin-B2 ligands (Fig. S4). The change in differentiation, therefore, was not due to the quantity of ephrin-B2 available. Additionally, the length scale associated with the spatial mutations was on the order of microns, which is far larger than the nanoscale dimensions of molecular interactions. Hence, molecular-scale clustering of ligand-receptor complexes were likely not disrupted even in the smallest grids. In all corrals, visible microclusters formed, and proximal signaling data revealed that known EphB4-ephrin-B2 induced-phosphorylation cascades were unaffected (Fig. 4 *E*). In particular, we examined pan-phosphorylated-tyrosine and known EphB4-ephrin-B2 signaling targets, including phosphorylated-ERK and active β-catenin. Furthermore, as is evident from Fig. 4 *D*, the cell footprints are of similar size across variable grid sizes. Because the grids are substantially smaller in scale than the cell, ligands will not gather from outside the cell footprint. Thus, we conclude that the total amount of ligand exposed to the cells remained unchanged by varying grid size.

In summary, we observe a clear effect from physically restricting the movement and assembly of EphB4-ephrin-B2 signaling clusters on NSC differentiation. Although the observed EphB4-ephrin-B2 clusters on all patterned substrates were apparently sufficient to induce downstream activation of several targets (Fig. 4 *E*), it is possible that restricting cluster size and microscale spatial organization on the cell membrane impacts downstream signaling. We have shown that increased oligomerization on the nanoscale induces higher levels of neurogenesis (23), but the role of microscale clustering remains undetermined. Alternatively, we have shown that the mechanical properties of the cellular microenvironment regulate NSC differentiation (56), and mechanical forces could conceivably play a role in the observed behavior. That is, the spatial mutation method utilized here intrinsically imposes mechanical forces on the receptor-ligand complexes, and a number of studies have demonstrated mechanical regulation of transmembrane receptors due to physical properties of ligand presentation, such as lateral mobility (57,58) and tugging forces at cell-cell junctions (59). Future work may explore the relative roles in biochemical and/or biomechanical signaling in mediating the effects of spatiomechanical perturbations on downstream NSC behaviors.

SUPPORTING MATERIAL

Supporting Materials and Methods, five figures, and two videos are available at http://www.biophysj.org/biophysj/supplemental/S0006-3495(18)30818-X.

Please cite this article in press as: Dong et al., Spatiomechanical Modulation of EphB4-ephrin-B2 Signaling in Neural Stem Cell Differentiation, Biophysical Journal (2018), https://doi.org/10.1016/j.bpj.2018.06.031

AUTHOR CONTRIBUTIONS

M.D., D.P.S., D.V.S., and J.T.G. designed research. M.D., D.P.S., and J.K.C. performed research. Y.K.L. and C.-H.Y. fabricated gridded substrates. M.D., D.P.S., and J.K.C. analyzed data. M.D., D.P.S., D.V.S., and J.T.G. wrote the manuscript.

ACKNOWLEDGMENTS

This work was supported, in part, by a grant from the National Cancer Institute of the National Institutes of Health under Grant U01CA202241 and National Institutes of Health under Grant R01NS083856.

REFERENCES

1. Himanen, J. P., N. Saha, and D. B. Nikolov. 2007. Cell-cell signaling via Eph receptors and ephrins. *Curr. Opin. Cell Biol.* 19:534–542.
2. Lisabeth, E. M., G. Falivelli, and E. B. Pasquale. 2013. Eph receptor signaling and ephrins. *Cold Spring Harb. Perspect. Biol.* 5:a009159.
3. Cayuso, J., Q. Xu, and D. G. Wilkinson. 2015. Mechanisms of boundary formation by Eph receptor and ephrin signaling. *Dev. Biol.* 401: 122–131.
4. Klein, R., and A. Kania. 2014. Ephrin signalling in the developing nervous system. *Curr. Opin. Neurobiol.* 27:16–24.
5. Barquilla, A., and E. B. Pasquale. 2015. Eph receptors and ephrins: therapeutic opportunities. *Annu. Rev. Pharmacol. Toxicol.* 55:465–487.
6. Pasquale, E. B. 2010. Eph receptors and ephrins in cancer: bidirectional signalling and beyond. *Nat. Rev. Cancer.* 10:165–180.
7. Davis, S., N. W. Gale, …, G. D. Yancopoulos. 1994. Ligands for EPH-related receptor tyrosine kinases that require membrane attachment or clustering for activity. *Science.* 266:816–819.
8. Stein, E., A. A. Lane, …, T. O. Daniel. 1998. Eph receptors discriminate specific ligand oligomers to determine alternative signaling complexes, attachment, and assembly responses. *Genes Dev.* 12:667–678.
9. Janes, P. W., B. Griesshaber, …, M. Lackmann. 2011. Eph receptor function is modulated by heterooligomerization of A and B type Eph receptors. *J. Cell Biol.* 195:1033–1045.
10. Schaupp, A., O. Sabet, …, R. Klein. 2014. The composition of EphB2 clusters determines the strength in the cellular repulsion response. *J. Cell Biol.* 204:409–422.
11. Janes, P. W., E. Nievergall, and M. Lackmann. 2012. Concepts and consequences of Eph receptor clustering. *Semin. Cell Dev. Biol.* 23:43–50.
12. Paszek, M. J., C. C. DuFort, …, V. M. Weaver. 2014. The cancer glycocalyx mechanically primes integrin-mediated growth and survival. *Nature.* 511:319–325.
13. Das, D. K., Y. Feng, …, M. J. Lang. 2015. Force-dependent transition in the T-cell receptor β-subunit allosterically regulates peptide discrimination and pMHC bond lifetime. *Proc. Natl. Acad. Sci. USA.* 112: 1517–1522.
14. Manz, B. N., B. L. Jackson, …, J. Groves. 2011. T-cell triggering thresholds are modulated by the number of antigen within individual T-cell receptor clusters. *Proc. Natl. Acad. Sci. USA.* 108:9089–9094.
15. Biswas, K. H., K. L. Hartman, …, J. T. Groves. 2015. E-cadherin junction formation involves an active kinetic nucleation process. *Proc. Natl. Acad. Sci. USA.* 112:10932–10937.
16. Bethani, I., S. S. Skånland, …, A. Acker-Palmer. 2010. Spatial organization of transmembrane receptor signalling. *EMBO J.* 29:2677–2688.
17. Salaita, K., P. M. Nair, …, J. T. Groves. 2010. Restriction of receptor movement alters cellular response: physical force sensing by EphA2. *Science.* 327:1380–1385.
18. Greene, A. C., S. J. Lord, …, J. T. Groves. 2014. Spatial organization of EphA2 at the cell-cell interface modulates trans-endocytosis of ephrinA1. *Biophys. J.* 106:2196–2205.
19. Chumley, M. J., T. Catchpole, …, M. Henkemeyer. 2007. EphB receptors regulate stem/progenitor cell proliferation, migration, and polarity during hippocampal neurogenesis. *J. Neurosci.* 27:13481–13490.
20. Holmberg, J., A. Armulik, …, J. Frisén. 2005. Ephrin-A2 reverse signaling negatively regulates neural progenitor proliferation and neurogenesis. *Genes Dev.* 19:462–471.
21. Nomura, T., C. Göritz, …, J. Frisén. 2010. EphB signaling controls lineage plasticity of adult neural stem cell niche cells. *Cell Stem Cell.* 7:730–743.
22. Ashton, R. S., A. Conway, …, D. V. Schaffer. 2012. Astrocytes regulate adult hippocampal neurogenesis through ephrin-B signaling. *Nat. Neurosci.* 15:1399–1406.
23. Conway, A., T. Vazin, …, D. V. Schaffer. 2013. Multivalent ligands control stem cell behaviour in vitro and in vivo. *Nat. Nanotechnol.* 8:831–838.
24. Zhang, C. L., Y. Zou, …, R. M. Evans. 2008. A role for adult TLX-positive neural stem cells in learning and behaviour. *Nature.* 451:1004–1007.
25. Blurton-Jones, M., M. Kitazawa, …, F. M. LaFerla. 2009. Neural stem cells improve cognition via BDNF in a transgenic model of Alzheimer disease. *Proc. Natl. Acad. Sci. USA.* 106:13594–13599.
26. Sahay, A., K. N. Scobie, …, R. Hen. 2011. Increasing adult hippocampal neurogenesis is sufficient to improve pattern separation. *Nature.* 472:466–470.
27. Balu, D. T., and I. Lucki. 2009. Adult hippocampal neurogenesis: regulation, functional implications, and contribution to disease pathology. *Neurosci. Biobehav. Rev.* 33:232–252.
28. Deng, W., J. B. Aimone, and F. H. Gage. 2010. New neurons and new memories: how does adult hippocampal neurogenesis affect learning and memory? *Nat. Rev. Neurosci.* 11:339–350.
29. Chrencik, J. E., A. Brooun, …, P. Kuhn. 2006. Structural and biophysical characterization of the EphB4*ephrinB2 protein-protein interaction and receptor specificity. *J. Biol. Chem.* 281:28185–28192.
30. Baksh, M. M., C. Dean, …, J. T. Groves. 2005. Neuronal activation by GPI-linked neuroligin-1 displayed in synthetic lipid bilayer membranes. *Langmuir.* 21:10693–10698.
31. Pautot, S., H. Lee, …, J. T. Groves. 2005. Neuronal synapse interaction reconstituted between live cells and supported lipid bilayers. *Nat. Chem. Biol.* 1:283–289.
32. Mossman, K. D., G. Campi, …, M. L. Dustin. 2005. Altered TCR signaling from geometrically repatterned immunological synapses. *Science.* 310:1191–1193.
33. Yu, C. H., and J. T. Groves. 2010. Engineering supported membranes for cell biology. *Med. Biol. Eng. Comput.* 48:955–963.
34. Groves, J. T. 2006. Spatial mutation of the T cell immunological synapse. *Curr. Opin. Chem. Biol.* 10:544–550.
35. Groves, J. T., N. Ulman, and S. G. Boxer. 1997. Micropatterning fluid lipid bilayers on solid supports. *Science.* 275:651–653.
36. Groves, J. T., and S. G. Boxer. 2002. Micropattern formation in supported lipid membranes. *Acc. Chem. Res.* 35:149–157.
37. DeMond, A. L., K. D. Mossman, …, J. T. Groves. 2008. T cell receptor microcluster transport through molecular mazes reveals mechanism of translocation. *Biophys. J.* 94:3286–3292.
38. Nair, P. M., K. Salaita, …, J. T. Groves. 2011. Using patterned supported lipid membranes to investigate the role of receptor organization in intercellular signaling. *Nat. Protoc.* 6:523–539.
39. Nye, J. A., and J. T. Groves. 2008. Kinetic control of histidine-tagged protein surface density on supported lipid bilayers. *Langmuir.* 24:4145–4149.
40. Chandra, R. A., E. S. Douglas, …, M. B. Francis. 2006. Programmable cell adhesion encoded by DNA hybridization. *Angew. Chem. Int. Ed. Engl.* 45:896–901.

41. Coyle, M. P., Q. Xu, …, J. T. Groves. 2013. DNA-mediated assembly of protein heterodimers on membrane surfaces. *J. Am. Chem. Soc.* 135:5012–5016.
42. Engin, S., V. Trouillet, …, D. Wedlich. 2010. Benzylguanine thiol self-assembled monolayers for the immobilization of SNAP-tag proteins on microcontact-printed surface structures. *Langmuir.* 26:6097–6101.
43. Keppler, A., S. Gendreizig, …, K. Johnsson. 2003. A general method for the covalent labeling of fusion proteins with small molecules in vivo. *Nat. Biotechnol.* 21:86–89.
44. Groves, J. T., R. Parthasarathy, and M. B. Forstner. 2008. Fluorescence imaging of membrane dynamics. *Annu. Rev. Biomed. Eng.* 10:311–338.
45. Knight, J. D., M. G. Lerner, …, J. J. Falke. 2010. Single molecule diffusion of membrane-bound proteins: window into lipid contacts and bilayer dynamics. *Biophys. J.* 99:2879–2887.
46. Moran, U., R. Phillips, and R. Milo. 2010. SnapShot: key numbers in biology. *Cell.* 141:1262–1262.e1261.
47. Himanen, J. P., K. R. Rajashankar, …, D. B. Nikolov. 2001. Crystal structure of an Eph receptor-ephrin complex. *Nature.* 414:933–938.
48. Hartman, N. C., J. A. Nye, and J. T. Groves. 2009. Cluster size regulates protein sorting in the immunological synapse. *Proc. Natl. Acad. Sci. USA.* 106:12729–12734.
49. Dustin, M. L., and J. T. Groves. 2012. Receptor signaling clusters in the immune synapse. *Annu. Rev. Biophys.* 41:543–556.
50. Xu, Q., W. C. Lin, …, J. T. Groves. 2011. EphA2 receptor activation by monomeric Ephrin-A1 on supported membranes. *Biophys. J.* 101: 2731–2739.
51. Xiao, Z., R. Carrasco, …, D. A. Tice. 2012. EphB4 promotes or suppresses Ras/MEK/ERK pathway in a context-dependent manner: implications for EphB4 as a cancer target. *Cancer Biol. Ther.* 13:630–637.
52. Williams, S. E., F. Mann, …, M. Henkemeyer. 2003. Ephrin-B2 and EphB1 mediate retinal axon divergence at the optic chiasm. *Neuron.* 39:919–935.
53. Cortina, C., S. Palomo-Ponce, …, E. Batlle. 2007. EphB-ephrin-B interactions suppress colorectal cancer progression by compartmentalizing tumor cells. *Nat. Genet.* 39:1376–1383.
54. Allonby, O., A. M. El Zawily, …, A. Freywald. 2014. Ligand stimulation induces clathrin- and Rab5-dependent downregulation of the kinase-dead EphB6 receptor preceded by the disruption of EphB6-Hsp90 interaction. *Cell. Signal.* 26:2645–2657.
55. Qin, H., R. Noberini, …, J. Song. 2010. Structural characterization of the EphA4-Ephrin-B2 complex reveals new features enabling Eph-ephrin binding promiscuity. *J. Biol. Chem.* 285:644–654.
56. Saha, K., A. J. Keung, …, K. E. Healy. 2008. Substrate modulus directs neural stem cell behavior. *Biophys. J.* 95:4426–4438.
57. Tsai, J., and L. C. Kam. 2010. Lateral mobility of E-cadherin enhances Rac1 response in epithelial cells. *Cell. Mol. Bioeng.* 3:84–90.
58. Narui, Y., and K. Salaita. 2013. Membrane tethered delta activates notch and reveals a role for spatio-mechanical regulation of the signaling pathway. *Biophys. J.* 105:2655–2665.
59. Liu, Z., J. L. Tan, …, C. S. Chen. 2010. Mechanical tugging force regulates the size of cell-cell junctions. *Proc. Natl. Acad. Sci. USA.* 107:9944–9949.